JPn Neuroscience

The Journal of Physiology

J Physiol 590.16 (2012) pp 4061–4077

Colour and pattern selectivity of receptive fields in superior colliculus of marmoset monkeys

Chris Tailby[1,2], Soon Keen Cheong[1,3], Alexander N. Pietersen[1,3], Samuel G. Solomon[2,4] and Paul R. Martin[1,3,4]

[1] *ARC Centre of Excellence in Vision Science, University of Sydney, 8 Macquarie St, Sydney, New South Wales 2001, Australia*
[2] *Brain Research Institute, Florey Neuroscience Institutes (Austin), 245 Burgundy St Heidelberg, Victoria 3084, Australia*
[3] *Save Sight Institute, University of Sydney, 8 Macquarie St, Sydney, New South Wales 2001, Australia*
[4] *Discipline of Physiology, University of Sydney, Building F13, Sydney, New South Wales 2006, Australia*

Key points

- In addition to supplying signals for conscious visual perception, the pathways from eye to brain serve visual functions such as reflex eye movements, which are controlled by a brain area called the superior colliculus (SC).
- It is known that short-wavelength sensitive (S or 'blue') cone photoreceptors serve an evolutionary ancient pathway for colour vision but whether S cones also contribute to reflex eye movements is poorly understood.
- We show that in recordings from anaesthetised marmoset monkeys, S cones do not contribute to visual responses in the SC. Thus, although S cones are a primitive part of the visual system their signals are selectively directed to thalamo-cortical pathways serving colour vision.
- The result also implies that colour-selective responses reported in SC of awake monkeys must arrive through indirect (non-retinal) inputs to the SC.

Abstract The main subcortical visual targets of retinal output neurones (ganglion cells) are the parvocellular and magnocellular layers of the dorsal lateral geniculate nucleus (LGN) in the thalamus. In addition, a small and heterogeneous collection of ganglion cell axons projects to the koniocellular layers of the LGN, to the superior colliculus (SC), and to other subcortical targets. The functional (receptive field) properties and target specificity of these non-parvocellular, non-magnocellular populations remain poorly understood. It is known that one population of koniocellular layer cells in the LGN (blue-On cells) receives dominant functional input from short-wavelength sensitive (S or 'blue') cones. Here we asked whether SC neurones also receive S cone inputs. We made extracellular recordings from single neurones ($n = 38$) in the SC of anaesthetised marmoset monkeys. Responses to drifting and flashed gratings providing defined levels of cone contrast were measured. The SC receptive fields we recorded were often binocular, showed 'complex cell' like responses (On–Off responses), strong bandpass spatial frequency tuning, direction selectivity, and many showed strong and rapid habituation to repeatedly presented stimuli. We found no evidence for dominant S cone input to any SC neurone recorded. These data suggest that S cone signals may reach cortical pathways for colour vision exclusively through the koniocellular division of the lateral geniculate nucleus.

(Received 14 February 2012; accepted after revision 6 June 2012; first published online 11 June 2012)
Corresponding author P. R. Martin: Save Sight Institute C09, University of Sydney, NSW 2006, Australia.
Email: prmartin@sydney.edu.au

Abbreviations: DI, direction index; EEG, electroencephalogram; K, koniocellular; LGN, lateral geniculate nucleus; M, magnocellular; ML, medium-long wavelength sensitive; OI, orientation index; P, parvocellular; PSTH, peristimulus time histogram; S, short wavelength sensitive; SC, superior colliculus; SF, spatial frequency; TF, temporal frequency.

DOI: 10.1113/jphysiol.2012.230409

Introduction

The superior colliculus (SC) is a laminated sensory-motor nucleus in the caudal midbrain involved in the coordination of head and eye movements. Superficial layers of the SC receive input from the retina; the deeper layers contain pre-motor neurones that participate in the control of gaze. The present study concerns the visual response properties of the superior colliculus (SC), in particular, the presence or absence of short wavelength sensitive (S or 'blue') cone input to the SC.

Early recordings from anaesthetised monkeys indicated that SC neurones and their retinal afferents lack input from S cones (Marrocco & Li, 1977; Schiller & Malpeli, 1977; DeMonasterio, 1978*b*,*c*). Recent recordings from awake behaving monkeys, however, showed that SC neurones are responsive to chromatic modulation. The colour-selective responses are seen at longer latency than responses to luminance modulations (White *et al.* 2009), which may indicate that colour selective signals arrive via an indirect (cortico-tectal) pathway whereas luminance information reaches the SC via a direct (retino-tectal) pathway. Accordingly, psychophysical studies show that S cone activation can influence eye movements, but does so at longer latencies than luminance modulations ('gap' and 'remote distractor' effects: Sumner *et al.* 2002, 2006; Anderson & Carpenter, 2008; Bompas & Sumner, 2009).

Anatomically, it has been estimated that about 10% of all primate retinal ganglion cells project to the SC (Perry & Cowey, 1984). The degree to which the SC projection comprises branches of axons innervating other subcortical visual centres has not been clearly established. Early studies found little overlap of retinal projections to the dorsal lateral geniculate nucleus (LGN) and the SC (Leventhal *et al.* 1981; Perry & Cowey, 1984; Perry *et al.* 1984; Rodieck & Watanabe, 1993) but more recent evidence implies axons of at least two ganglion cell classes (parasol and smooth monostratified) branch to innervate both LGN and SC (Crook *et al.* 2008*a*,*b*). There is no evidence that the retinal projection to SC includes the well-characterised 'blue-On/small bistratified' cell, but the SC projection does includes sparsely branched cells (Rodieck & Watanabe, 1993) with morpology linked to blue-Off responses (Dacey *et al.* 2003). These anatomical results raise the possibility that blue-Off signals travel directly from the retina to the SC. Such signals should arrive at short latency and be detectable in anaesthetised animals. The goal of the present study is to test this prediction.

In the early studies cited above, adapting fields were used to suppress one or more cone channels and an action spectrum was then obtained with narrow-band lights. The relative weight of inputs from different cone classes is difficult to establish where adapting backgrounds are used, and therefore measurements using cone-selective stimulation (Derrington *et al.* 1984; Conway, 2001; Sun *et al.* 2006*a*; Field *et al.* 2007; Tailby *et al.* 2008*b*) are now preferred and are used in the current study.

In broad context the pattern and colour selectivity of receptive fields in the koniocellular (K) layers of the dorsal lateral geniculate nucleus, in the SC, and in other subcortical retinal targets remain poorly understood. Many K receptive fields in diurnal (macaque and marmoset) monkeys show strong S cone input (Schiller & Malpeli, 1978; Martin *et al.* 1997; Tailby *et al.* 2008*a*; Roy *et al.* 2009), but other K receptive fields in marmosets (and all K cells in nocturnal monkeys) lack S cone inputs completely (Xu *et al.* 2001; Levenson *et al.* 2007). The question of S cone signals in the retino-tectal projection bears both on the nature of the S cone input to the human gaze control system, and on the degree of heterogeneity in non-standard retinal projections.

Methods

Ethical approval

Marmosets (*Callithrix jacchus*, $n = 3$) were obtained from the Australian National Health and Medical Research Council (NHMRC) combined breeding facility. Procedures were approved by the institutional (University of Melbourne and University of Sydney) Animal Experimentation and Ethics Committee, and conform to the Society for Neuroscience and NHMRC policies on the use of animals in neuroscience research.

Experimental preparation

Each animal was initially anaesthetised with an intramuscular injection of 12 mg kg^{-1} Alfaxan (Jurox, NSW, Australia) and 3 mg kg^{-1} Diazepam (Roche, NSW, Australia). We then gave preoperative intramuscular injections of 0.2 mg kg^{-1} atropine (Pfizer, NSW, Australia), to reduce lung secretions, and dexamethasone (0.3 mg kg^{-1}; Maine Pharmaceuticals, VIC, Australia) to reduce inflammation. Subsequent surgery was performed with supplemental local anaesthesia (lignocaine 2%; AstraZeneca, NSW, Australia) and supplemental doses of Alfaxan. A femoral vein or tail vein was cannulised, the trachea exposed and an endotracheal tube inserted. The head was placed in a stereotaxic frame, and a craniotomy made over the SC (centred at stereotactic coordinates 0 mm antero-posterior and ∼2 mm lateral to midline). Post-surgical anaesthesia was maintained by continuous intravenous infusion of sufentanil citrate (4–12 μg kg^{-1} h^{-1}; Sufenta Forte, Janssen Cilag, Beerse, Belgium) in physiological solution (sodium lactate, Baxter International, NSW, Australia) with added dexamethasone (0.4 kg^{-1} h^{-1}; Mayne Pharma, VIC, Australia) and Synthamin 17 (225 kg^{-1} h^{-1}; Baxter

International, NSW, Australia). Neuromuscular blockade was then induced and maintained by continuous infusion of pancuronium bromide ($0.3\,kg^{-1}\,h^{-1}$; AstraZeneca, NSW, Australia). The animal was artificially ventilated so as to keep end-tidal CO_2 near 4.5%.

Electroencephalogram (EEG) and electrocardiogram signals were monitored to ensure adequate depth of anaesthesia. The EEG signal was subjected to Fourier analysis. Dominance of low frequencies (1–5 Hz) in the EEG recording, and absence of EEG changes under noxious stimulus (tail-pinch) were taken as the chief sign of an adequate level of anaesthesia. We found that low dose rates in the range cited above were always very effective during the first 24 h of recordings. Thereafter, drifts towards higher frequencies (5–10 Hz) in the EEG record were counteracted by increasing the rate of venous infusion or the concentration of anaesthetic. The typical duration of a recording session was 48–72 h.

Rectal temperature was kept near 38°C with the use of a heating blanket. Additional antibiotic, and anti-inflammatory cover was given daily by intramuscular injection of 25 mg penicillin (Norocillin, Norbrook, UK), and 0.1 mg dexamethasone. The pupils were dilated with atropine sulphate and the corneas were protected with high-permeability contact lenses that remained in place for the duration of the experiment. No artificial pupils were used. Supplementary lenses (with power determined by maximising the spatial resolution of the first receptive fields encountered for each eye) were used to focus the eyes at a distance of 114 cm.

A small incision was made in the dura and a guide tube containing a recording electrode was inserted and positioned above the superior colliculus. Measurements were obtained using paralyene-coated tungsten electrodes (Frederick Haer Co., Bowdoinham, ME, USA, impedence 9–12 MΩ). In two of the animals (case MY138 and case MY139) we made preliminary recordings from the LGN prior to the SC recordings, and the purpose of these recordings was to determine the animals' colour vision phenotype as described below.

Visual stimulus and single cell recording

A front-silvered mirror was used to bring the receptive field onto the centre of a cathode ray tube monitor (ViewSonic G810, 100 Hz refresh rate; or Sony G520, refresh rate 120 Hz or 120.4 Hz). Optical path length from the monitor screen to the pupil plane was 114 cm. Visual stimuli were generated by a G5 Power Macintosh computer using custom software (Expo; P. Lennie); stimuli were drawn with 8-bit resolution using commands to OpenGL. For each phosphor we determined the relationship between the output of the video card and the photopic luminance; the inverse of this relationship was applied to the signals that were sent to the video card.

A set of spectral absorbance templates (nomograms) with peak wavelengths corresponding to those present in each animal was generated using a polynomial template (Lamb, 1995). The effect of receptor self-screening was estimated assuming axial absorbance of 1.5% and outer segment length 20 μm. Lens absorbance was corrected using published measurements for marmoset (Tovée *et al.* 1992). The contrast in a given class of cone generated by each stimulus was obtained by calculating the inner product between the relevant cone nomogram and the spectral power distribution of the (linearized) R, G and B guns specified by the stimulus. The resulting inner products (corresponding to cone activations elicited separately by the R, G and B guns) were then summed and expressed relative to their values at the white point (R, G and B guns set to the mean value), calculated in the same manner. The spectral power distribution of each gun was determined with a PR-650 photometer (Photo Research, Palo Alto, CA, USA). The absorption spectra of the different subtypes of marmoset cone are not known as precisely as those of the human, and the profile of macular pigment density in this species is also uncertain. We did not correct for macular pigment as all receptive fields were located more than one degree from the foveola (mean eccentricity = 10 deg; min = 2.5 deg; max = 19.8 deg). We refer to stimulus conditions as S cones selective and medium-long wavelength sensitive (ML) cone selective, but it is of course possible that variations in pre-receptoral absorption make these stimuli deviate slightly from the optimal cone selective colour directions. In other words, perfect cone isolating stimuli are theoretically ideal but impossible to achieve in practice. Our approach to this problem is to generate stimuli which minimize the inevitable deviations and use appropriate controls to allow proper interpretation of deviations on recorded responses. The effect of deviations depends on the sign and magnitude of cone inputs to the receptive field under study. In theory, for example, spurious ML contrast could act to cancel S cone inputs to a 'blue/yellow' opponent receptive field. In practice however deviations from optimal cone-isolating conditions are much more likely to produce spurious, albeit weak, positive inputs from nominally silenced cones. In previous work we demonstrated that 'bleed-through' of signals from nominally silent cones is an important consideration in recordings from high gain cells such as magnocellular cells in the lateral geniculate nucleus (Tailby *et al.* 2008*b*); we dealt with the problem of distinguishing real from spurious cone inputs in ways described below. The nominal S cone-isolating stimulus produced 60–80% contrast in S cones and less than 5% contrast in the ML cones. The nominal ML cone-isolating stimulus produced

over 60% contrast in ML class cones and less than 2% contrast in S cones.

The ML cones expressed by each animal were determined as described in detail elsewhere (Blessing *et al.* 2004; Martin *et al.* 2011), by polymerase chain reaction/restriction fragment length polymorphism analysis of the ML opsin-encoding genes, or by analysis of responses to red-green heterochromatic modulation in recordings made from parvocellular cells in the lateral geniculate nucleus prior to the SC recordings. Two of the animals were dichromatic, expressing S cones (peak ∼423 nm) and a second cone class in the medium-long wavelength sensitive range peaking near 556 nm (case MY133), or 563 nm (case MY138). The trichromatic female (case MY139) expressed M and L cones at peaks of 543 nm and 556 nm.

The stimulus was a drifting sinusoidal grating, or a uniform field modulated in time; all stimuli modulated around the mean luminance (45–55 cd m^{-2}) and were presented within a circular window with hard edges, outside which the screen (20 deg × 15 deg) was held at the mean luminance. For each cell, the optimal spatial frequency, temporal frequency, orientation and contrast was determined, using achromatic drifting gratings. Receptive fields were binocular in all cells in which this was tested; for expediency we presented stimuli monocularly to the dominant eye in nearly all cases. An aperture-tuning curve was measured using the optimum stimulus parameters. An aperture diameter that was slightly above the optimal diameter, and that contained at least one full cycle of the preferred spatial frequency, was used thereafter. The analogue signals from the electrodes were amplified, filtered and sampled at 48 kHz by the same computer that generated the visual stimulus. Putative spikes were displayed on a monitor and templates for discriminating spikes were constructed by analysing multiple traces. The timing of waveforms that cohered to the template was recorded with an accuracy of 0.1 ms. Off-line analysis was performed using Matlab (The MathWorks, Natick, MA, USA).

Response was calculated from the discharge recorded during the initial 500 ms of each stimulus presentation. During this period, some cells in the superior colliculus responded to a drifting stimulus with unmodulated elevation of the discharge ('F0'), whereas others showed periodic modulation of their discharge at the frequency of stimulation ('F1'; see Fig. 1). For a given cell we determined which response measure to use ('F0' *vs.* 'F1') by calculating the variance of F0 responses and F1 responses for all presented stimuli; the metric with higher variance across stimuli (thus, the greatest differential response) was used.

In most cells we measured response as a function of drift direction for full contrast gratings of otherwise optimised parameters. We quantified direction selectivity by calculating a direction index (DI):

$$\mathrm{DI} = \left| \frac{\sum \vec{v}_i}{\sum |r_i|} \right|,$$

where v_i are vectors pointing in the direction of the stimulus and having length r_i, equal to the response recorded during that stimulus, relative to the response to a stimulus of 0% contrast (Vaney & Taylor, 2002). The DI can range from 0, when the responses are equal for all stimulus directions, to 1, when a response is obtained only for a single stimulus direction. Values approaching 1 therefore indicate responses increasingly concentrated around a preferred direction. An orientation index (OI) was calculated in equivalent manner by doubling the angle of each direction vector in the equation.

Location of recorded cells

The position of each recorded cell was noted by reading the depth from the hydraulic microelectrode advance (David Kopf Model 640). Electrolytic lesions (6–10 μA × 6–10 s, electrode negative) were made to mark selected recording positions. At the termination of the recording session the animal was killed with an overdose of pentobarbitone sodium (80–150 mg kg^{-1}, Lethabarb; Verbac Australia, NSW, Australia) administered through the intravenous catheter.

Recording position in the superior colliculus was confirmed histologically (White *et al.* 2001; Szmajda *et al.* 2006). We did not systematically reconstruct the laminar position of cells encountered, but note that that most cells (61%, 23 of 38) were encountered within 300 μm of encountering the superficial surface of the superior colliculus (mean 294 μm, SD 267, $n = 38$). No systematic differences in the response properties reported below were seen on comparing receptive fields encountered at different recording depths.

Results

We describe here data collected from 38 neurones recorded from 18 electrode penetrations in the superior colliculus (SC) of two females and one male marmoset. During electrode penetrations we routinely presented S cone isolating gratings as 'lure' stimuli to maximise the probability of encountering cells with strong S cone inputs. In total, 57 locations in SC were recorded; recordings from 16 locations were rejected because of poor single-cell isolation; data from three further neurones with low response rates (<5 imp s^{-1}) were not included in the following analyses.

Spatiotemporal tuning within SC

Figure 1 illustrates receptive field properties of a neurone in the SC. The left panels of Fig. 1*A*–*C* show responses to stimulation of the contralateral (right) eye; right panels show responses to stimulation of the ipsilateral (left) eye. In each panel the mean rate of discharge (F0) and the amplitude of the component of the discharge modulated at the stimulus temporal frequency (F1) are shown. Spatiotemporal tuning is broadly similar in the two eyes. The right eye receptive field prefers a direction near 240 deg and the left eye prefers close to the opposite direction near 60 deg. The weak responses to right eye stimulation (Fig. 1*A*) are primarily due to the use of a stimulus direction more suited to the left eye. We did not explore binocular direction tuning on a cell-by-cell basis, so we do not know how representative the binocular responses are of SC neurones as a population. We return to the question of monocular direction biases in a later section. Figure 1*D* and *E* show a drawing and 50 μm coronal section through the midbrain of the marmoset at the level of the superior colliculus, processed with Nissl stain (cresyl violet). The black arrow identifies an

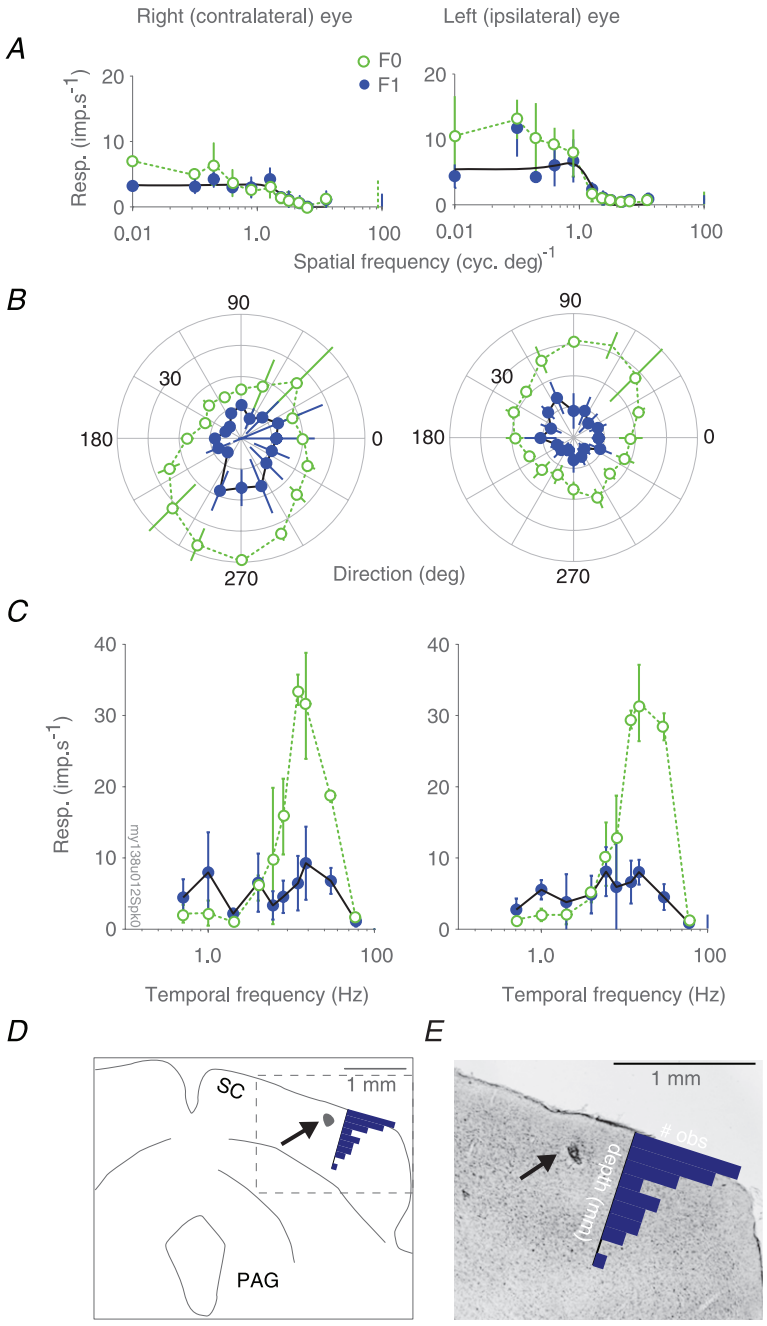

Figure 1. Example recordings from a neurone recorded in, and electrolytic lesion created by recording electrode in, marmoset superior colliculus
A–*C*, spatial frequency (*A*), direction (*B*), and temporal frequency (*C*) tuning curves measured in response to stimulations through either the contralateral (left column) or the ipsilateral (right column) eye of a visually responsive neurone in marmoset superior colliculus. Open green symbols show F0 response; filled blue symbols show F1 response; vertical lines at the rightmost *x*-axis limits show spontaneous activity; error bars report standard deviation. Smooth black lines in *A* show the difference of Gaussians model that best fits the F1 responses. Stimulus parameters for panel *A*: grating drift direction 145 deg, drift rate 5Hz, aperture diameter 4 deg. *D*–*E*, drawing (*D*) of coronal section (*E*) through the midbrain of the marmoset at the level of the superior colliculus, processed with Nissl stain (cresyl violet). Dashed box in *D* shows the region displayed in *E*. Black arrow points to electrolytic lesion. The overlay histograms show the encounter position of recorded neurones relative to the (dorsoventral) position where visually driven multiunit activity was observed. PAG: periaqueductal grey; SC: superior colliculus.

electrolytic lesion created by the recording electrode at the end of the recording session to confirm recording location in the superior colliculus.

In the following sections our initial focus is on comparison of SC receptive fields with receptive fields in the lateral geniculate nucleus (LGN). We first show that (in contrast to responses in LGN) response of SC neurones to drifting gratings are usually rectified, and show habituation over the 1–2 s duration of each trial. We then show that SC neurones respond to temporal square wave S cone modulation, as previously shown in awake primate SC (White *et al.* 2009) and anaesthetised monkey LGN (Tailby *et al.* 2008*a*,*b*). We analyse these putative S cone inputs to SC and show that they likely arise from residual ML cone contrast rather than genuine S cone inputs. Finally we describe orientation and direction selectivity in SC.

Habituation and rectification in SC responses

Figure 2*A*, *B*, *D* and *E* shows the peri-stimulus time histograms (PSTHs) of four SC neurones in the 500 ms preceding, and during the first second following, presentation of a full contrast achromatic grating drifting at 5 cycle s^{-1}. Stimulus onset is at time 0 on the *x*-axis. Before stimulus onset the screen was uniform grey. The small red squares immediately above the *x*-axis denote the temporal period of the drifting grating. The discharge of two of the cells (Fig. 2*A* and *B*) is modulated at the frequency of the stimulus (F1), with a clear peak in the discharge occurring

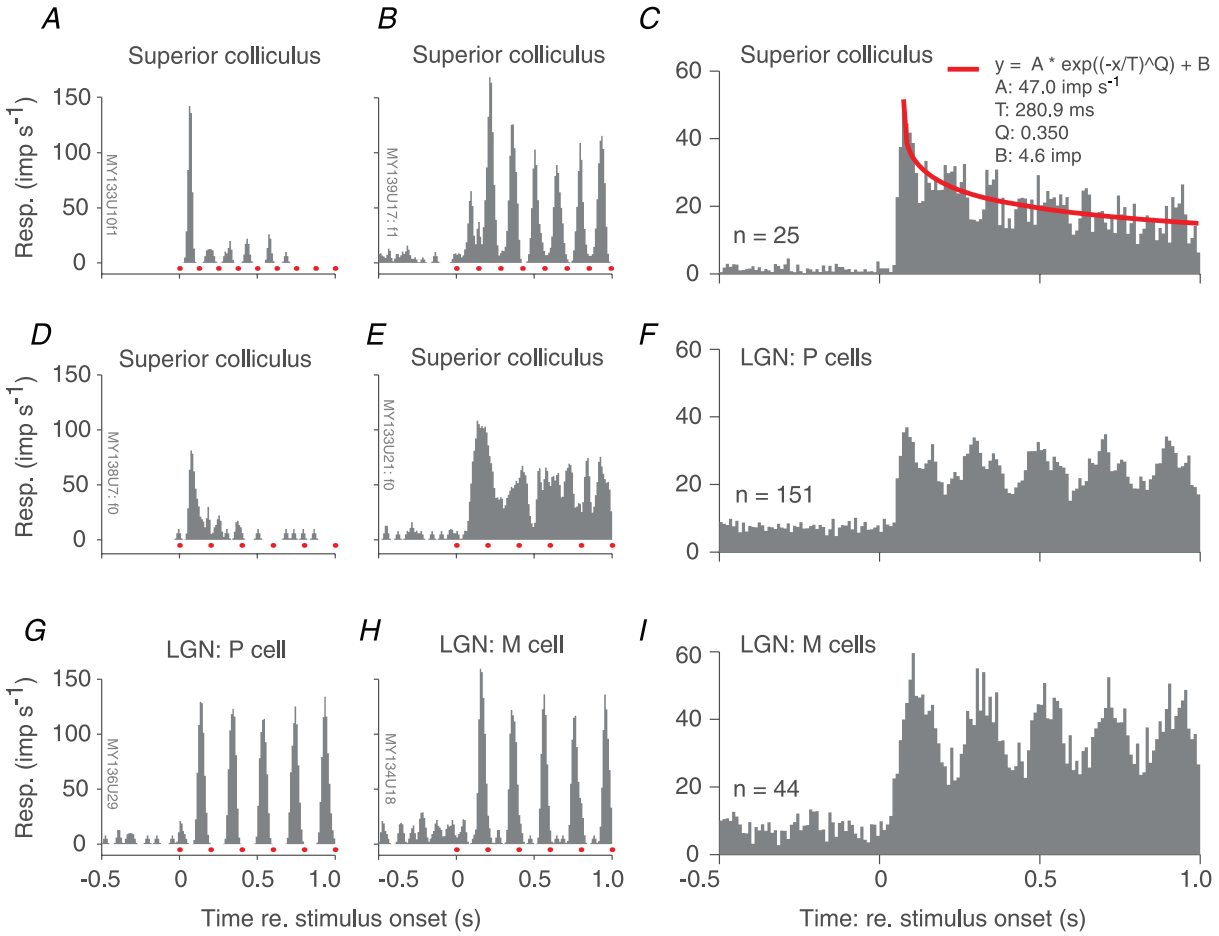

Figure 2. Nature of visual response in marmoset superior colliculus: example cells
A, *B*, *D* and *E*, peri-stimulus time histograms (PSTHs) obtained from four different marmoset superior colliculus (SC) neurones during the 500 ms preceding and 1000 ms following the onset of a drifting achromatic grating (red dots immediately above *x*-axis indicate the temporal period of the grating). During the interval preceding grating onset (at time = 0) the animal viewed a uniform grey screen of the same mean luminance as the grating. Responses are dominated either by the F1 (*A* and *B*) or F0 (*D* and *F*) component, and are either relatively transient (*A* and *D*) or sustained (*B* and *E*). *C*, population average PSTH for a sample of SC neurones. Stimulus temporal frequency and spatial phase varied across cells, so no period markers are provided. Red continuous line shows best fit of stretched exponential decay function. *F* and *I*, PSTHs obtained from example parvocellular (*F*) and magnocellular (*I*) neurones recorded in marmoset lateral geniculate nucleus (LGN).

once per cycle of drift. By contrast, the discharge of the cells shown in Fig. 2*D* and *E* are dominated by elevation in the mean discharge (F0). Forty-six per cent of the cells (17/37) in our sample were classified as 'F1' cells according to the criteria described in Methods. (One cell was only tested with flashed gratings, so we were unable to classify it as F0 or F1.)

As well as differing in the nature of their response to the drifting stimulus (F0 *vs.* F1), the cells in Fig. 2*A*, *B*, *D* and *E* also differ in the degree to which their response habituates during maintained stimulus presentation. For the two cells in Fig. 2*A* and *D* there is a strong response transient, after which response decays rapidly. Conversely, for the cells in Fig. 2*B* and *E* the response is sustained throughout the 1 s stimulus period. Across all cells in our sample, the median habituation (response rate in 40–200 ms after stimulus onset, divided by response rate in 700–1000 ms after stimulus onset) was 1.7. Figure 2*G* and *H* shows PSTHs for example parvocellular (P) and magnocellular (M) cells recorded in the LGN. The LGN data were reanalysed from our previous studies (Szmajda *et al.* 2006; Tailby *et al.* 2008*b*). For both LGN cell types, the discharge is modulated at the stimulus frequency, and responses do not habituate over the 1 s duration of stimulus exposure (see also Camp *et al.* 2011).

Figure 2*C* shows the population average of PSTHs in response to a full contrast drifting achromatic grating. In the averaged responses the time-locked modulation of the PSTH is reduced because stimulus temporal frequency and response latency differed between cells. For comparison, Fig. 2*F* and *I* shows the average PSTH obtained for P and M cells in the LGN; here the lack of habituation is obvious. The residual PSTH modulation in LGN is also more prominent than in SC; this is because the LGN neurones showed much more consistent and tight phase-locking to the 5 Hz drifting gratings used for the initial stages of cell characterisation.

We conclude from the above analysis that many SC neurones show rectified responses or habituate rapidly to drifting grating stimuli. We allowed for these facts in our data analysis in two ways. Firstly, we note that both weakly and strongly habituating neurones are active during the first 500 ms following stimulus onset (cf. Fig. 2*C*, Fig. 2*A* and *D*). We therefore analysed SC responses over the first 500 ms following stimulus onset. Secondly, we defined response as either the mean discharge (relative to the maintained rate; F0, $n = 20$ cells) across this 500 ms epoch, or the amplitude of the modulation of the discharge at the stimulus frequency (F1, $n = 17$ cells), using criteria described in Methods.

Compared to F1 cells, F0 cells tended to have higher contrast sensitivity, higher preferred spatial frequency (SF), higher cut-off SF, and more low pass temporal tuning, but these trends were weak and only the difference in temporal frequency (TF) low cut ratio ([response to lowest TF measured]/[response to preferred TF]) was statistically significant (Mann–Whitney *U* test, $P < 0.02$). Maximum response rates, spatial frequency tuning (low frequency attenuation), preferred TFs, and TF resolution of the F1 and F0 groups were comparable, so responses were pooled for further analysis.

SC cells respond to flashed S cone isolating stimuli

The principal aim of this paper is to examine the question of S cone input to the SC. We first approached this question during our initial characterisation of cells, by measuring responses to slow (0.5 Hz) square wave temporal modulation (flashes) of a uniform field that either modulated all cones in phase (achromatic), or the S cones in isolation. The flashed stimulus is similar to that used by White *et al.* (2009) to identify isoluminant responses in SC of awake macaques.

Previous studies of monkey superior colliculus show rectified responses to flashed stimuli, that is a flashed stimulus elicited spike bursts at both light onset and offset (Schiller & Koerner, 1971; Schiller & Stryker, 1972). Figure 3*A* shows average response of 17 SC neurones that responded to square wave temporal modulations (six additional neurones exposed to these stimuli did not respond reliably). Of the 17 cells, 12 responded with a transient increase in discharge at each transition

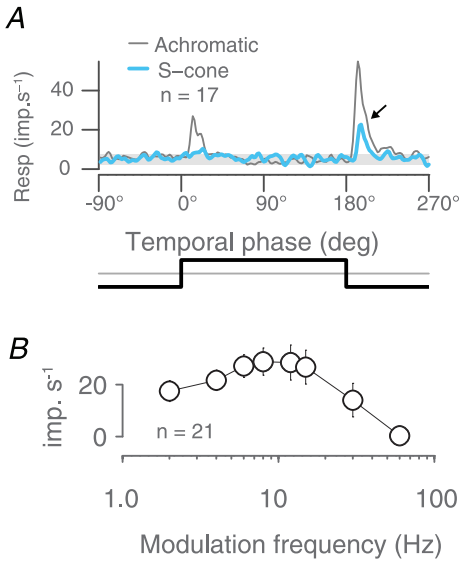

Figure 3. Population average response to slow, square wave modulation of a large uniform field
A, superior colliculus population average response to two cycles of 0.5 Hz square wave temporal modulation of an achromatic (thin grey trace) or S cone selective (thick blue trace) uniform field. Note response to offset of S cone modulation (arrow). The temporal profile of the stimulus is illustrated below the graph. *B*, population average temporal frequency tuning for drifting achromatic gratings. Error bars show standard errors of the mean.

in the achromatic stimulus (light-to-dark, and dark-to-light), indicating that they were of On–Off response type; the remaining five cells responded with a transient increase in discharge at the light-to-dark transition, indicating that they were Off-response type. Even among the On–Off cells the Off-response was much stronger than the On-response. In other words, the asymmetry of the On- and Off-responses in the population average is not an artefact of averaging different response types.

For the S cone isolating stimulus we observed a transient population response to S cone decrements (Fig. 3*A*); this response appears delayed by ~7 deg (~10 ms at 0.5 Hz) relative to that to the achromatic stimulus. The delayed S cone response was apparent in both On–Off and Off-cells, and among the On–Off cells an S cone response was

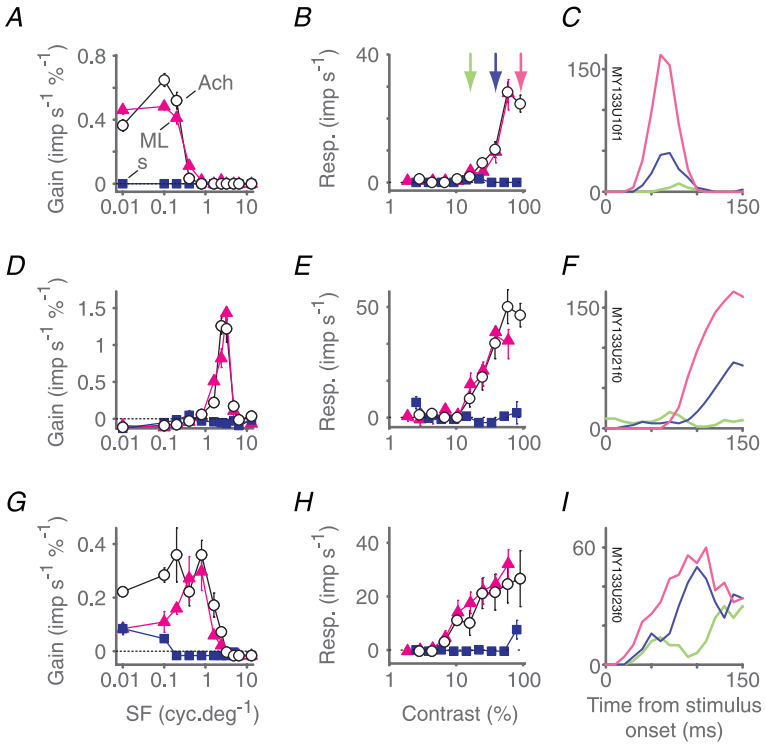

Figure 4. Selectivity of cone inputs to superior colliculus revealed via spatial and contrast tuning: example cells
A–C, spatial frequency tuning (*A*) and contrast response (*B*) of a superior colliculus neurone for drifting achromatic (open circles), ML cone selective (magenta triangles) and SWS cone selective (blue squares) gratings. *C*, PSTH recorded over the first 150 ms following onset of a drifting achromatic grating or varying contrast (constructed from data shown in *B*). The discharge of the cell is modulated at the frequency of stimulation (F1). Colour code in *C* indicates grating contrast as identified by *x*-axis location of the corresponding collared vertical line in *B*. Error bars (sometimes concealed by data points) show standard errors of the mean. *D–F*, same as *A–C* but for a cell in which stimulation primarily induced an elevation in the mean rate of discharge (F0). *G–I*, same as *A–C* but for another cell in which stimulation primarily induced an elevation in the mean rate of discharge (F0). This cell shows the strongest indication of SWS cone input (at low spatial frequencies) of all the cells in our sample. Baseline responses (maintained discharge) have been subtracted from amplitude graphs.

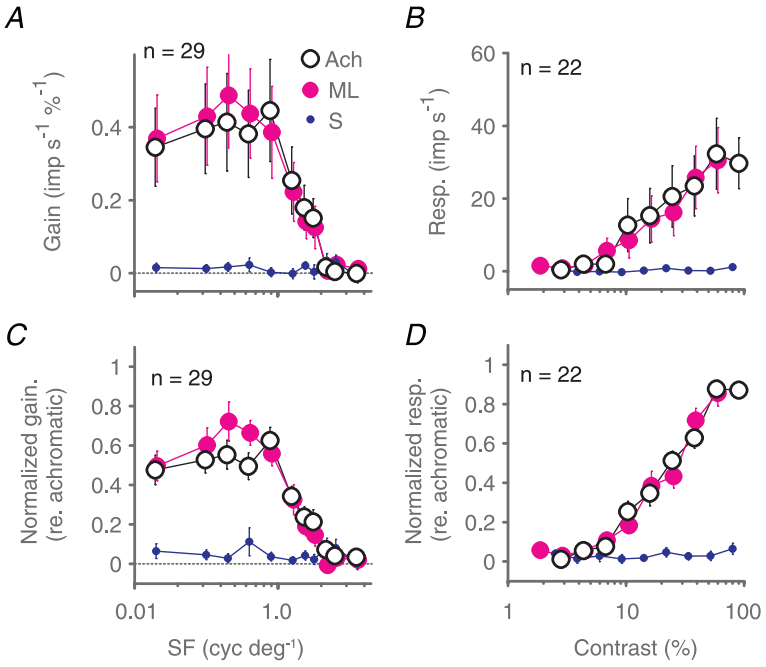

Figure 5. Selectivity of cone inputs to superior colliculus revealed via spatial and contrast tuning: population average
A and *B*, population average spatial frequency tuning (*A*) and contrast response (*B*) calculated across our sample of 29 superior colliculus neurones for drifting achromatic (open symbols), ML cone selective (large magenta symbols) and SWS cone selective (small blue symbols) gratings. *C* and *D*, same as *A* and *B* but prior to averaging across cells, each individual cell's tuning curve was normalized to its maximum achromatic response. Normalization was done separately for spatial frequency and contrast data. Data show that the achromatic tuning curves are almost completely explained by the ML tuning curves, with no contribution from SWS cones. Error bars show standard errors of the mean; *n* listed in each panel identifies the number of neurones contributing to the population average. Baseline responses (maintained discharge) have been subtracted from amplitude graphs.

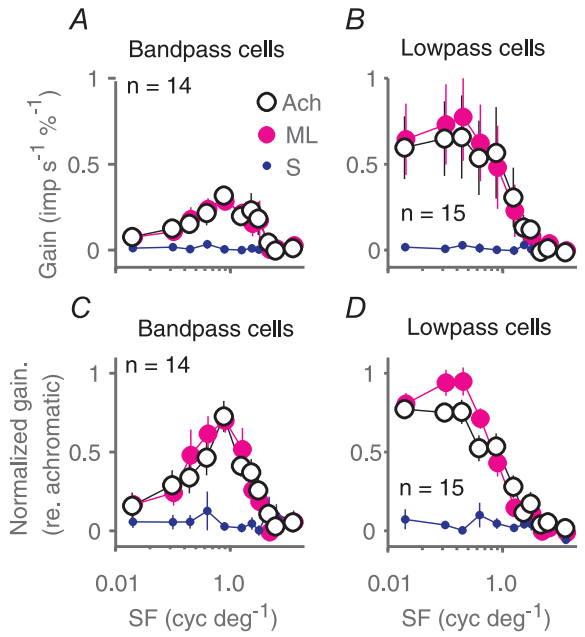

Figure 6. Comparison of cone inputs to bandpass and lowpass superior colliculus neurones
A and *C*, population average raw (*A*) and normalized (*D*) spatial frequency tuning for drifting achromatic (large open symbols), ML cone selective (large magenta symbols) and SWS cone selective (small blue symbols) gratings; calculated for bandpass superior colliculus neurones ([response to lowest SF]/[response to best SF] < 0.5). *B* and *D*, same as *A* and *C* but calculated only for lowpass neurones ([response to lowest SF]/[response to best SF] ≥ 0.5). Error bars show standard errors of the mean; *n* listed in each panel identifies the number of neurones contributing to the population average. Baseline responses (maintained discharge) have been subtracted from amplitude graphs.

only apparent for S cone decrements. These properties resemble the isoluminant responses of the neurones in the superficial layers of the SC reported by White *et al.* (2009). In the following we analyse response to drifting gratings, and find support for the suggestion by White *et al.* (2009) that isoluminant responses in superficial layers of SC are not due to S cone inputs but result from luminance artefacts.

Absence of response to drifting S cones gratings in superior colliculus

Figure 3*B* gives an important clue to understanding why SC cells respond to both achromatic and S cone isolating flashed fields, that is SC cells show high responsivity for a wide range of temporal frequencies in drifting achromatic gratings. The broad temporal and spatial frequency spectrum of flashed edges could thus be a potent stimulus for SC neurones. We therefore proceeded to measure contrast and spatial frequency transfer properties of SC neurones. Figure 4*A*, *D* and *G* shows the responses of three SC neurones to achromatic, ML cone isolating, and S cone isolating drifting gratings varying in spatial frequency. Responses are expressed as gain (imp s^{-1} $\%^{-1}$) so as to factor out the different effective cone contrasts of each stimulus chromaticity. All three cells show comparable tuning for achromatic and ML stimuli, and little or no response to S cone isolating gratings. Figure 4*B*, *E* and *H* shows contrast response curves at optimum spatial frequency, and Figure 4*C*, *F* and *I* shows response to one stimulus cycle at different achromatic contrasts. The tuning of the cell in Fig. 4*A*–*C* resembles that of typical M cells in the LGN: spatial frequency tuning is moderately bandpass (Fig. 4*A*), there is response saturation at high contrasts (Fig. 4*B*), and responses at high contrast are phase advanced relative to responses at low contrast (Fig. 4*C*). The cell in Fig. 4*D*–*F* is however distinct from most LGN receptive fields in that its spatial frequency tuning is completely bandpass (a property reminiscent of cortical visual neurones). Neither neurone responds to selective modulation of the S cones. These two neurones are representative of the majority of cells we encountered in SC. The third cell, shown in Fig. 4*G*, *H* and *I*, showed the strongest response of any cell in our sample to S cone isolating stimuli. The achromatic and ML isolating spatial frequency tuning curves were slightly different, particularly at low spatial frequencies, and responses to S cone isolating modulations were apparent at the lowest frequencies. The cell was very sensitive to achromatic and ML cone contrast, but responded to S cones contrast only at the highest contrast presented (80%).

Figure 5 shows population average responses in the same format as shown in Fig. 4. The upper panels show population averages derived from raw responses; the lower panels show responses relative to the maximum achromatic response for each cell. In each panel, achromatic and ML isolating curves overlap almost perfectly, and responses to S cones stimuli are negligible. Thus, at the population level, responses within the SC are unaffected by modulation of the S cones.

The responses of the cells shown in Fig. 4 suggest substantial variation in spatial frequency selectivity between cells. Low-pass spatial tuning is characteristic of blue-On and blue-Off cells in LGN (Wiesel & Hubel, 1966; Szmajda *et al.* 2006; Tailby *et al.* 2008*a*,*b*); we therefore repeated our population analysis with cells segregated into groups with strong and weak surrounds. The cells were categorised by their response to the lowest spatial frequency tested, expressed as a fraction of their response to the preferred spatial frequency; with a criterion value of 0.5. The result is shown in Fig. 6, which confirms that average tuning functions of both low pass and band pass spatial frequency-tuned cells lack S cone input. The same result was obtained when a criterion of 0.8 was used.

We have previously presented evidence that high ML cone contrast sensitivity probably underlies the

weak responses to nominal S cone isolating modulation sometimes observed in M cells in marmoset LGN (Tailby *et al.* 2008*b*). This explanation, however, seems unlikely for the SC neurone shown in Fig. 4*E* and *F*: its spatial frequency tuning for S cone modulation is low pass, whereas that for ML cone and achromatic modulation is band pass. This raises the question whether, given the size of our sample, we might reliably expect to have detected weak S cone inputs if they are present in the SC. We approached this question by performing bootstrap analyses of our laboratories' existing databases of P and M cells in LGN, where S cone inputs are only present in a minority of neurones. For each of 1000 bootstrap resamples we randomly drew, with replacement, a sample of LGN spatial frequency and contrast tuning curves, and calculated the average response to pure S cone modulation and to modulation of the ML cones (in some cells this was pure ML modulation; in others, achromatic modulation). Figure 7*A* and *B* shows the resulting mean and 95% confidence interval of LGN tuning curves drawn exclusively from P cells; Fig. 7*C* and *D* shows the same analysis for LGN M cells. These data show that the population average responses to S cone modulation in SC neurones are comparable or slightly lower than those of P cells, and significantly lower than those in M cells. These data indicate that responses to S cone isolating gratings in SC are comparable to those observed among retinal P ganglion cells (where S cone inputs are undetectable: Sun *et al.* 2006*b*) or LGN P cells (where S cone inputs are rare: Tailby *et al.* 2008*b*).

Quantitative comparison of S cone weights in LGN and primary visual cortex

The foregoing results in combination with our previous studies (White *et al.* 1998; Hashemi-Nezhad *et al.* 2008; Szmajda *et al.* 2008; Tailby *et al.* 2008*b*) imply that S cone signals are not widely distributed to subcortical targets but (where measured so far) are functionally segregated to the koniocellular layers of the LGN. In Fig. 8 we have quantified this segregation. Here, we compare the functional weight of S cone inputs to SC neurones with our previous estimates of S cone weight to neurones in LGN (Hashemi-Nezhad *et al.* 2008; Tailby *et al.* 2008*b*) and primary visual cortex. Figure 8*A*–*E* show scatterplots and marginal histograms of relative S cone weight (S/[S + ML]) obtained in the current study (SC, Fig. 8*A*) and reanalysed from our previous studies of V1 (Hashemi-Nezhad *et al.* 2008; Tailby *et al.* 2008*b*) and LGN (pooled data from Tailby *et al.* 2008*b*; Hashemi-Nezhad *et al.* 2008): M cells (Fig. 8*C*); blue-On and blue-Off cells (Fig. 8*D*); PC cells (Fig. 8*E*). Cone weights to SC neurones were estimated from ML and S cone isolating tuning curves at the peak ML spatial frequency for each neurone. For each panel the *y*-axis shows measured S cone weight, and the *x*-axis shows the prediction of a simple 'random connections' model where the weight is determined simply by the local proportion of S cones at the visual field eccentricity of the recorded neurone, as explained in detail in our previous studies. The two main conclusions we draw from this analysis are firstly that the functional weight of inputs to S cone cells (blue-On and blue-Off) in the LGN

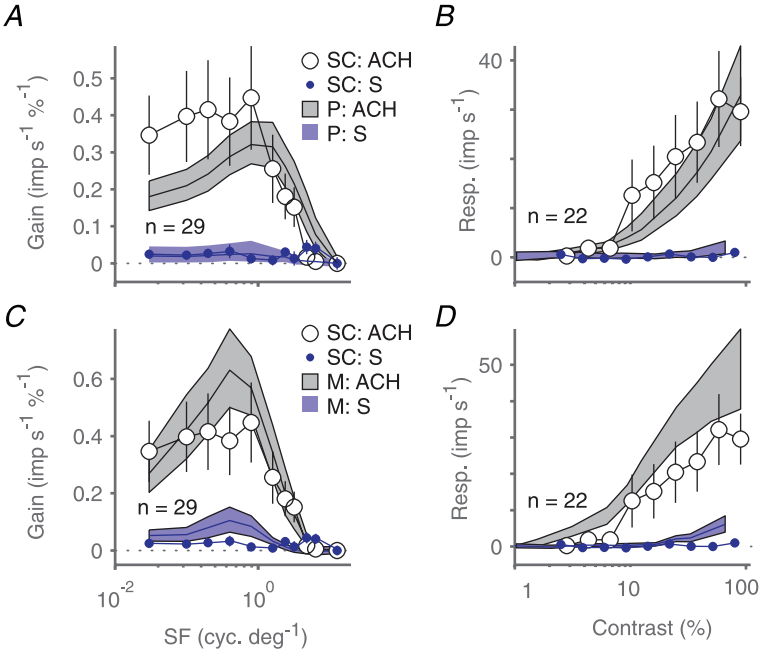

Figure 7. Comparison of the relative strength of S cone inputs to superior colliculus (SC) neurones and to neurones in lateral geniculate nucleus (LGN)
A and *B*, population average spatial frequency (*A*) and contrast (*B*) tuning of SC neurones for drifting achromatic gratings (large open circles) and SWS cone selective gratings (small blue symbols); data are reproduced from Fig. 5*A*. Filled grey (upper) and dashed blue (lower) polygons show bootstrapped mean and 95% confidence intervals for the equivalent population tuning of parvocellular (P) LGN neurones. *C* and *D*, same as *A* and *B* but comparison is now with magnocellular (M) LGN neurones. Error bars show standard errors of the mean; *n* listed in each panel identifies the number of superior colliculus neurones contributing to the population average, and the number of P and M neurones drawn from our LGN database on each bootstrap resample. Baseline responses (maintained discharge) have been subtracted from amplitude graphs.

is substantially higher than the weight of inputs to any other cell class, and secondly that there is heavy overlap of S cone weight among all 'non-blue' classes of neurone studied (Fig. 8*F* shows, on magnified scale, the range of observed and predicted S cone inputs to the non-blue populations for comparison). In summary, rather than contributing in a non-specific way to subcortical targets, the S cone signals in the areas we have measured so far are tightly segregated to specific populations of blue-On and blue-Off neurones which contribute to koniocellular pathways (White *et al.* 1998; Szmajda *et al.* 2006, 2008; Roy *et al.* 2009).

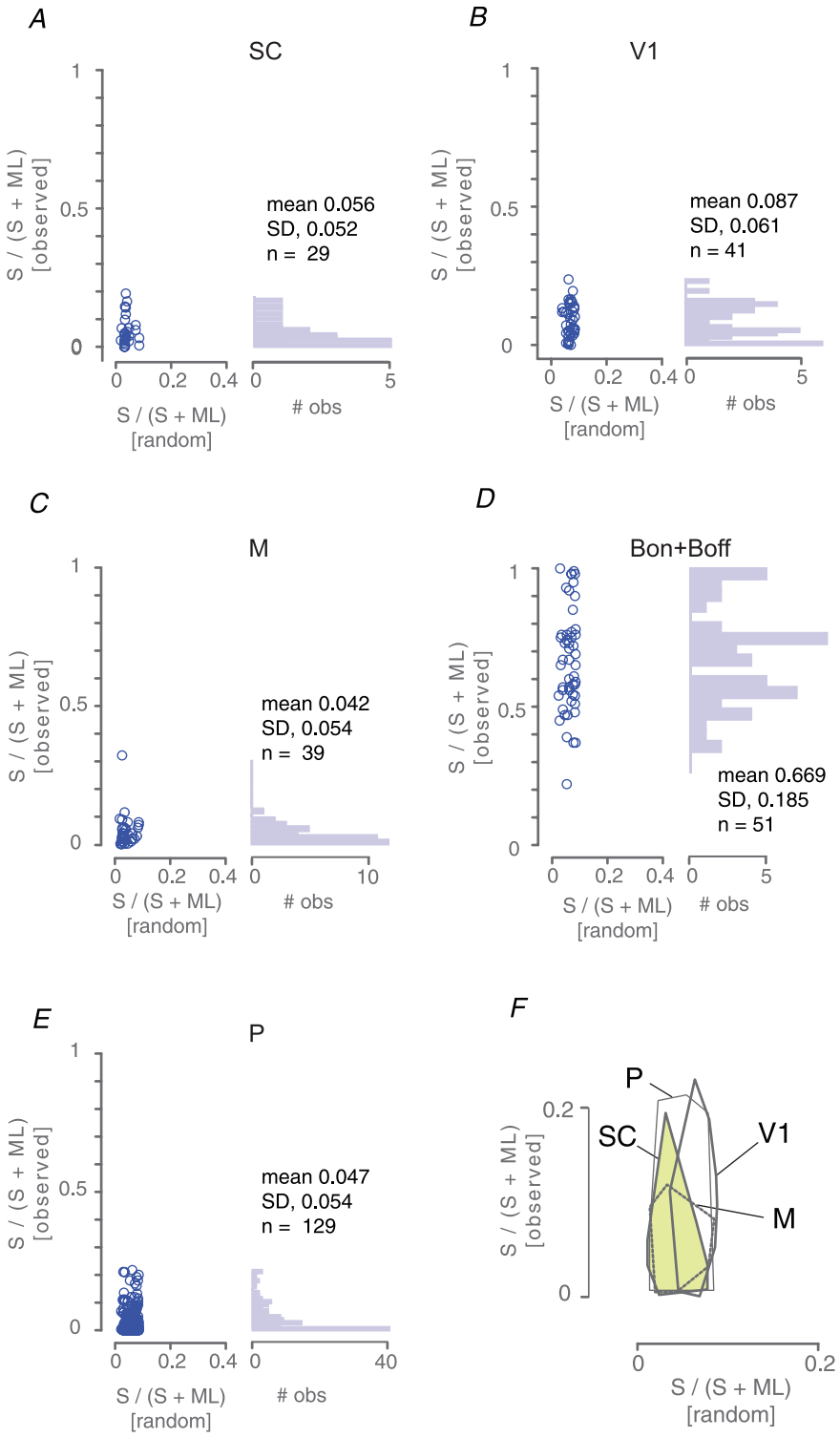

Figure 8. Summary of S cone signal strength in subcortical targets and primary visual cortex
Panels *A*–*E* show scatterplots and marginal histograms of relative S cone weight (*S*/[S + ML]) obtained in superior colliculus (SC, panel *A*), primary visual cortex (V1, panel *B*) and three populations in lateral geniculate nucleus: magnocellular cells (M, panel *C*); blue-On and blue-Off cells (Bon + Boff, panel *D*); parvocellular cells (P, panel *E*). For each panel the *y*-axis show measured S cone weight, and the *x*-axis shows the prediction of a simple 'random connections' model where the weight is determined simply by the local proportion of S cones at the visual field eccentricity of the recorded neurone . Panel *F* shows, at enlarged scale, convex hull outlines of the non-blue populations. Note heavy overlap of these distributions. One outlier M cell (cf. panel *C*) was not included in the convex hull. V1 data re-analysed from Hashemi-Nezhad *et al.* (2008). LGN data pooled from the current study and two of our previous studies (Hashemi-Nezhad *et al.* 2008; Tailby *et al.* 2008*b*).

Direction tuning in superior colliculus neurones

We observed direction bias in many SC neurones. Initial reports indicated that visually responsive neurones in primate SC lack direction selectivity (Schiller & Koerner, 1971; Cynader & Berman, 1972; Schiller & Stryker, 1972; Marrocco & Li, 1977; Moors & Vendrik, 1979; Davidson & Bender, 1991). Other work showed some neurones in monkey SC are selective for the direction of motion of visual stimuli (Goldberg & Wurtz, 1972; Horwitz & Newsome, 1999), though it has been suggested that these responses result from operant conditioning on eye-movement contingent tasks (Horwitz *et al.* 2004). Given the presence of direction selective neurones in SC of cat (Sterling & Wickelgren, 1969; Wickelgren & Sterling, 1969; Ogasawara *et al.* 1984), and recent reports of direction biases among some K pathway neurones (Forte *et al.* 2005; Tailby *et al.* 2008*a*,*b*), we therefore were interested to characterise direction selectivity in marmoset SC.

Figure 9*A*–*C* shows direction-tuning curves for three SC cells. Illustrated are tuning curves for cells with direction indices (DIs, see Methods) corresponding to low (Fig. 9*A*), average (Fig. 9*B*), and high (Fig. 9*C*) values. Some cells were orientation tuned but not direction tuned (e.g. Fig. 9*A*), whereas other cells were strongly direction tuned and responses were suppressed below the maintained discharge rate if stimuli drifted in the anti-preferred direction (Fig. 9*C*). Figure 9*D* shows the population average direction-tuning curve for our sample of SC neurones. Responses are normalised and referred to direction of maximal response. The population average direction-tuning curve has a DI of 0.1. The mean DI across cells in our sample was 0.17 (SD 0.2; median: 0.12). These values are comparable to that measured in marmoset blue-On cells (geometric mean: ∼0.13), and substantially higher than reported for in LGN P cells and M cells (median: ∼0.03) (see Tailby *et al.* 2010). Fifty-six per cent of SC neurones (18/32) had DI $>$ 0.1. In Fig. 9*E* we plot DI against the orientation index (OI, see Methods), along with marginal histograms (Fig. 9*F*,*G*). These data indicate a large proportion of SC neurones in marmosets shows mild orientation bias, but few SC neurones are strongly biased for direction.

Discussion

We observed no evidence of dominant S cone input to the receptive fields of superior colliculus (SC) neurones recorded in anaesthetised marmosets. At the population level, the average response of our SC cell sample to S cone modulations was as weak or weaker than that of lateral geniculate nucleus (LGN) parvocellular (P) cells measured using exactly the same stimuli (Fig. 7, Fig. 8). A large body of work, in both macaque and marmoset, indicates that most P cells receive negligible S cone input (Derrington *et al.* 1984; Sun *et al.* 2006*a*; Hashemi-Nezhad *et al.* 2008; Tailby *et al.* 2008*a*,*b*). Our population average SC data therefore shows that the SC in anaesthetised marmoset lacks meaningful S cone input.

At first glance the temporal square wave data of Fig. 3*A* and the drifting grating data of Figs 4–7 seem to provide conflicting information regarding the question of S cone inputs to the SC. While the two stimulus protocols used comparable nominal S cones contrasts, the temporal frequency content of the stimuli is very different. A single temporal frequency dominates the drifting grating stimulus, but the temporal square wave stimulus includes power at frequencies much higher than those we used for the drifting gratings. The transient responses of the SC neurones to the step transitions in (Fig. 3*A*) are consistent with the idea that these cells prefer high temporal frequencies. Furthermore, cells showing higher ML cone response gain showed stronger responses to S cones step transitions (not shown). All these lines of evidence suggest that the S cone step responses reflect sensitivity to residual ML cone contrast in the nominal S cones stimulus, as investigated more extensively in our earlier work in marmoset LGN (Tailby *et al.* 2008*b*). Consistently, during the square wave temporal modulation, the latency of the S cone response appeared longer (by ∼10 ms) than that for achromatic modulation. The achromatic contrast response of SC neurones shows contrast-dependent phase advance (Fig. 4*C*, *F* and *I*). This is further evidence that the S cones step response may actually reflect a response to low ML contrast in the stimulus, a possibility further suggested by the association between ML cone contrast sensitivity and S cone step responsiveness. It is however important to note that that genuine S cone inputs from the retina could come at longer latencies than ML cone inputs if different retinal circuits process the S cone signals and/or the S cone signals are conducted by slower fibres than those that conduct ML cone signals.

It could be argued that in our recordings from SC we for some reason (e.g. electrode bias) did not encounter S cones recipient cells that were present. We note here, however, that we used exactly the same animal preparation, stimulus generation, and recording procedures that we have used previously in studies of LGN, where we have routinely encountered blue-on and blue-off cells, as illustrated in Fig. 8, as well as occasionally other rarely encountered cell types. We therefore think a systematic bias against S cone cells in our recordings is unlikely.

For each recorded neurone we attempted to characterise fully (given the limits of recording stability) the spatial frequency, orientation and temporal selectivity for S cone isolating, ML cone isolating, and achromatic drifting gratings. This procedure takes time, and limits the number of cells which can be characterised in each animal. An alternative approach would be to screen large

numbers of neurones then characterise in detail only cells showing substantial S cone input. The main difficulty with this approach is that many SC cells show substantial orientation and/or frequency selectivity (e.g. Figs 1*A* and *C*, 4*D* and 6*C*) making a general-purpose screening stimulus practically impossible to construct. The fact that many SC neurones showed complex-like properties and rapid habituation also renders reverse correlation or 'flickering checkerboard' methods impractical, because large numbers of spikes are required for covariance analysis: this stricture is incompatible with a rapid screening requirement. Furthermore as explained above and below ('Spatial receptive field properties of SC neurones') a broad-screen approach would preclude quantitative comparison of SC responses with our previous studies in LGN. In summary, we believe our systematic receptive field exploration using gratings is the best way to capture the diversity of receptive field properties in the SC and assess their cone inputs.

It could be argued that because short-wave cones are disproportionately vulnerable to toxins, hypoxia, drugs and dietary deficiencies, we did not record strong S cone signals in SC for the simple reason that functional S cones were not present in the recorded animals. For two animals (case MY138 and case MY139) we can rule out this possibility on functional grounds because we made preliminary recordings from the LGN in these animals, and in each case noted typical blue-On receptive fields. Furthermore in unrelated anatomical experiments (data not shown) the retinas of all three animals were processed

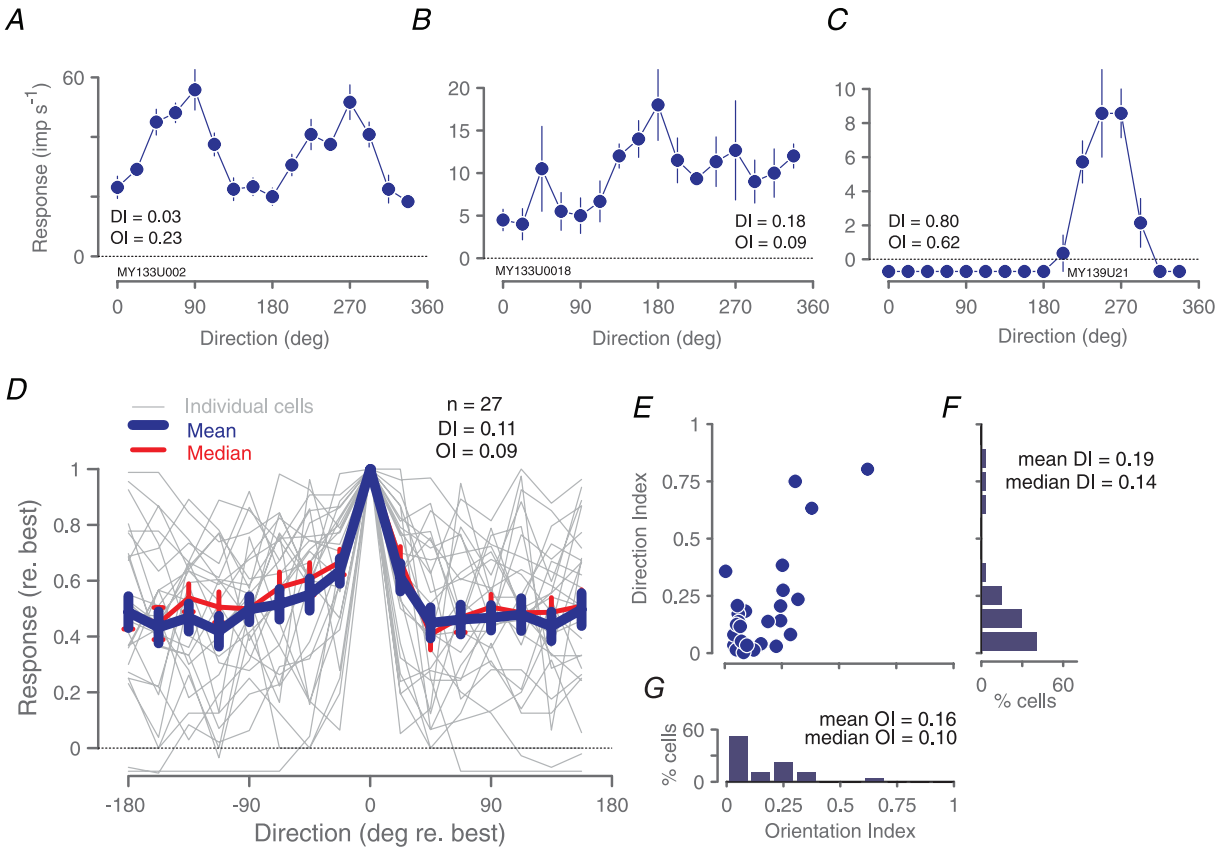

Figure 9. Direction tuning of superior colliculus neurones for drifting achromatic gratings
A–C, direction tuning curves for three example superior colliculus neurones: a moderately orientation tuned neurone (*A*), a moderately direction tuned neurone (*B*), and the most strongly direction tuned neurone in our sample (*C*). Error bars show standard errors of the mean; DI: direction index; OI: orientation index, calculated as explained in the text. *D*, population average (thick blue line) and median (thin red line) direction tuning curve of our sample of superior colliculus neurones; thin grey lines show individual direction tuning curves, demonstrating variability across cells. DI and OI refer to values calculated on the average curve (blue line). Data are aligned to the direction of maximal response and normalized to maximum response amplitude. Error bars show standard errors of the mean; *n* in panel identifies *D* the number of neurones contributing to the population average. *E*, scatterplot of DI against OI for the 27 cells in our sample. *F*, histogram of DI; mean and median DI calculated from the values obtained in individual cells (shown in *E*). *G*, histogram of OI; mean and median OI calculated from the values obtained in individual cells (shown in *E*). Baseline responses (maintained discharge) have been subtracted from amplitude graphs.

with antibodies against S cone opsin and the normal pattern of S cone staining was observed. We did not measure responses in LGN for the third animal (Case MY133). We have reviewed our records and found that in LGN recordings we have made from over 80 marmosets obtained from the same (closed) colony since 1996 we never failed to find blue-On cells in experiments where we were seeking them. On these bases the probability that case MY133 expressed a normal functional complement of S cones is high.

Effect of anaesthesia

White *et al.* (2009) show robust S cone signals in SC of awake behaving macaque monkeys, whereas our data indicate negligible S cone signals in SC of anaesthetised marmoset monkeys. This may reflect a species difference between macaque and marmoset monkeys, but according to the following line of argument is more likely to be attributable to anaesthetic state. The S cone signals observed in recordings from the SC of awake animals (White *et al.* 2009), and inferred from psychophysical studies of the saccadic system (Sumner *et al.* 2006; Anderson & Carpenter, 2008; Bompas & Sumner, 2009), come at longer latency (by at least 30 ms) than ML cone signals, consistent with an origin in non-retinotectal pathways. The majority of neurones we recorded were located in the superficial layers of SC and our population ($n = 38$) most likely overlaps with the 'transient-visual' and 'sustained-visual' populations ($n = 28$) recorded in superficial layers of awake macaques (White *et al.* 2009). These neurones show relatively weak and temporally delayed responses to coloured stimuli (White *et al.* 2009). Our results provide indirect support for White *et al.*'s (2009) hypothesis that the delayed chromatic responses they observe do not arise via a direct retinotectal projection, on the assumption that indirect inputs are less active in anaesthetised than in waking animals. The connections of superficial layers of SC with striate and extrastriate cortices give multiple potential routes for S cone signals to reach SC and descending cortico-tectal and cortico-thalamic pathways are likely to be facilitatory (reviewed by Gandhi & Sparks, 1966; Sherman & Guillery, 2006). In the most direct comparison attempted to date, visual thalamic (LGN) receptive fields show higher responsivity in awake behaving monkeys than in anaesthetised monkeys (Alitto *et al.* 2011); if this is also the case for SC fields then one would expect stronger S cone signals in awake than in anaesthetised animals.

Spatial receptive field properties of SC neurones

While the principal aim of this study was to characterise SC sensitivity to S cone modulations, in doing so we also collected data concerning other functional properties of SC receptive fields. We adopted this approach in order to keep our stimulus conditions most compatible with our previous studies in LGN (Szmajda *et al.* 2006; Tailby *et al.* 2008*a*,*b*) and primary visual cortex (Hashemi-Nezhad *et al.* 2008). We found that compared to thalamic (LGN) receptive fields the SC fields were often binocular, showed 'complex cell' like responses (On–Off responses), strong bandpass spatial frequency tuning, direction selectivity, and strong and rapid habituation.

Binocular receptive fields are rare in LGN (Cheong *et al.* 2010). While suppressive inputs from the non-dominant eye have been observed in M cells (Rodieck & Dreher, 1979), increases in spike rate are rarely evoked by stimuli presented to the non-dominant eye. In the present recordings from SC we informally observed that in all cells tested, presenting stimuli to either eye caused increases in spike rate. This observation is consistent with several previous studies (Schiller & Koerner, 1971; Cynader & Berman, 1972; Goldberg & Wurtz, 1972; Moors & Vendrik, 1979). In the one cell examined in detail, the preferred direction in the two eyes differed by ∼180 deg, corresponding to the retinal image motion that would be produced by a looming or a receding stimulus; a possible role for SC in detecting such stimuli has not to our knowledge been systematically studied.

Cells that are excited by both light increments and decrements, or respond to drifting sinusoidal gratings with an increase in the mean rate of discharge, are only rarely encountered in recordings from primate retina and LGN (DeMonasterio, 1978*c*; Casagrande, 1994; White *et al.* 2001; Petrusca *et al.* 2007; Tailby *et al.* 2007; Crook *et al.* 2008*a*; Solomon *et al.* 2010). Complex-cell like behaviour was exhibited by the majority (20/37) of SC cells in our sample, as has been reported previously (Schiller & Koerner, 1971; Cynader & Berman, 1972; Goldberg & Wurtz, 1972). When we grouped cells on the basis of the degree to which their discharge was modulated at the frequency of stimulation (F1/F0 ratio; Skottun *et al.* 1991), we found no reliable differences except that complex-like cells were more lowpass in their TF tuning, but there was substantial heterogeneity observed within each group. Curiously, in the current sample all cells that responded to square-wave temporal modulation of uniform fields were either On–Off response type (12/17) or Off-response type (5/17). We are unaware of such a bias in earlier studies of primate SC.

Rapid habituation in responses of SC neurones has been noted previously (Horn & Hill, 1966; Kadoya *et al.* 1971; Marrocco & Li, 1977); such behaviour is effectively absent from LGN populations measured in our and other laboratories. Similarly, very few retinal and LGN neurones exhibit complete bandpass spatial frequency selectivity. Indeed, bandpass spatial frequency selectivity is generally considered an emergent property of cortical neurones (DeValois *et al.* 1982; Webb *et al.* 2005). Direction

selectivity has previously been noted in ∼10% of SC neurones (Schiller & Koerner, 1971; Cynader & Berman, 1972; Goldberg & Wurtz, 1972; Horwitz & Newsome, 1999). Four of 27 SC neurones in our sample had direction indices in excess of 0.3 (i.e. strong direction selectivity). Our informal observation was that direction selectivity in SC is relatively stable in face of temporal and spatial frequency variation.

In summary, our data indicate a diverse range of functional properties in the SC. Many of these properties depart from the properties apparent in the majority of retinal ganglion cells. These complex properties may arise from retinal inputs in rare ganglion cell classes, by processing of simple input signals within the SC, or from non-retinal inputs to SC.

Relation of the SC to the koniocellular pathways and S cone signals

Our finding that SC receptive fields lack S cone inputs may seem surprising in light of anatomical evidence. Retinal inputs to the SC, and inputs to the koniocellular (K) layers of the LGN, include a variety of wide-field (non-M, non-P) ganglion cell types (Rodieck & Watanabe, 1993; Dacey *et al.* 2003; Szmajda *et al.* 2008). At least three of the wide-field ganglion cell types recieve functional input from S cones (Dacey & Packer, 2003; Dacey *et al.* 2003), and there is increasing evidence that many ganglion cell classes send axon branches both to the LGN and the SC (Dacey & Lee, 1994). Furthermore, the SC projects to the K layers of the LGN in all primates studied to date (Harting *et al.* 1991). Thus there are anatomical links between the K layers and the SC on one hand, and between the K layers and S cone signals on the other hand. However, the lack of clear S cone signals among our and others' recordings from SC (Marrocco & Li, 1977) and its retinal afferents (Schiller & Malpeli, 1977; DeMonasterio, 1978*a*,*c*) indicates that S cone signal carrying ganglion cells do *not* innervate the SC.

References

Alitto HJ, Moore BDt, Rathbun DL & Usrey WM (2011). A comparison of visual responses in the lateral geniculate nucleus of alert and anaesthetized macaque monkeys. *J Physiol* **589**, 87–99.

Anderson AJ & Carpenter RH (2008). The effect of stimuli that isolate S-cones on early saccades and the gap effect. *Proc Biol Sci* **275**, 335–344.

Blessing EM, Solomon SG, Hashemi-Nezhad M, Morris BJ & Martin PR (2004). Chromatic and spatial properties of parvocellular cells in the lateral geniculate nucleus of the marmoset (*Callithrix jacchus*). *J Physiol* **557**, 229–245.

Bompas A & Sumner P (2009). Oculomotor distraction by signals invisible to the retinotectal and magnocellular pathways. *J Neurophysiol* **102**, 2387–2395.

Camp AJ, Cheong SK, Tailby C & Solomon SG (2011). The impact of brief exposure to high contrast on the contrast response of neurons in primate lateral geniculate nucleus. *J Neurophysiol* **106**, 1310–1321.

Casagrande VA (1994). A third parallel visual pathway to primate area V1. *Trends Neurosci* **17**, 305–310.

Cheong SK, Lim JHK, Tailby C, Solomon SG & Martin PR (2010). Orientation selectivity in a subpopulation of neurones in the primate lateral geniculate nucleus. *2010 Abstract Viewer/Itinerary Planner*, Programme No. 276.13. Society for Neuroscience, Washington, DC.

Conway BR (2001). Spatial structure of cone inputs to color cells in alert macaque primary visual cortex (V-1). *J Neurosci* **21**, 2768–2783.

Crook JD, Peterson BB, Packer OS, Robinson FR, Gamlin PD, Troy JB & Dacey DM (2008*a*). The smooth monostratified ganglion cell: evidence for spatial diversity in the Y-cell pathway to the lateral geniculate nucleus and superior colliculus in the macaque monkey. *J Neurosci* **28**, 12654–12671.

Crook JD, Peterson BB, Packer OS, Robinson FR, Troy JB & Dacey DM (2008*b*). Y-cell receptive field and collicular projection of parasol ganglion cells in macaque monkey retina. *J Neurosci* **28**, 11277–11291.

Cynader M & Berman N (1972). Receptive-field organization of monkey superior colliculus. *J Neurophysiol* **35**, 187–201.

Dacey DM & Lee BB (1994). The 'blue-on' opponent pathway in primate retina originates from a distinct bistratified ganglion cell type. *Nature* **367**, 731–735.

Dacey DM & Packer OS (2003). Colour coding in the primate retina: diverse cell types and cone-specific circuitry. *Curr Opin Neurobiol* **13**, 421–427.

Dacey DM, Peterson BB, Robinson FR & Gamlin PD (2003). Fireworks in the primate retina: in vitro photodynamics reveals diverse LGN-projecting ganglion cell types. *Neuron* **37**, 15–27.

Davidson RM & Bender DB (1991). Selectivity for relative motion in the monkey superior colliculus. *J Neurophysiol* **65**, 1115–1133.

DeMonasterio FM (1978*a*). Center and surround mechanisms of opponent-color X and Y ganglion cells of retina of macaques. *J Neurophysiol* **41**, 1418–1434.

DeMonasterio FM (1978*b*). Properties of concentrically organized X and Y ganglion cells of macaque retina. *J Neurophysiol* **41**, 1394–1417.

DeMonasterio FM (1978*c*). Properties of ganglion cells with atypical receptive-field organization in retina of macaques. *J Neurophysiol* **41**, 1435–1449.

Derrington AM, Krauskopf J & Lennie P (1984). Chromatic mechanisms in lateral geniculate nucleus of macaque. *J Physiol* **357**, 241–265.

DeValois RL, Albrecht DG & Thorell LG (1982). Spatial frequency selectivity of cells in macaque visual cortex. *Vision Res* **22**, 545–559.

Field GD, Sher A, Gauthier JL, Greschner M, Shlens J, Litke AM & Chichilnisky EJ (2007). Spatial properties and functional organization of small bistratified ganglion cells in primate retina. *J Neurosci* **27**, 13261–13272.

Forte JD, Hashemi-Nezhad M, Dobbie WJ, Dreher B & Martin PR (2005). Spatial coding and response redundancy in parallel visual pathways of the marmoset *Callithrix jacchus*. *Visual Neurosci* **22**, 479–491.

Gandhi NJ & Sparks DL (1966). Changing views of the role of the superior colliculus in the control of gaze. In *The Visual Neurosciences*, ed. Chalupa LM & Werner JS, pp. 1449–1465. The MIT Press, Cambridge, MA.

Goldberg ME & Wurtz RH (1972). Activity of superior colliculus in behaving monkey. I. Visual receptive fields of single neurons. *J Neurophysiol* **35**, 542–559.

Harting JK, Huerta MF, Hashikawa T & van Lieshout DP (1991). Projection of the mammalian superior colliculus upon the dorsal lateral geniculate nucleus: organization of tectogeniculate pathways in nineteen species. *J Comp Neurol* **304**, 275–306.

Hashemi-Nezhad M, Blessing EM, Dreher B & Martin PR (2008). Segregation of short-wavelength sensitive ("blue") cone signals among neurons in the lateral geniculate nucleus and striate cortex of marmosets. *Vision Res* **48**, 2604–2614.

Horn G & Hill RM (1966). Responsiveness to sensory stimulation of units in the superior colliculus and subjacent tectotegmental regions of the rabbit. *Exp Neurol* **14**, 199–223.

Horwitz GD, Batista AP & Newsome WT (2004). Direction-selective visual responses in macaque superior colliculus induced by behavioral training. *Neurosci Lett* **366**, 315–319.

Horwitz GD & Newsome WT (1999). Separate signals for target selection and movement specification in the superior colliculus. *Science* **284**, 1158–1161.

Kadoya S, Wolin LR & Massopust LCJ (1971). Photically evoked unit activity in the tectum opticum of the squirrel monkey. *J Comp Neurol* **142**, 495–508.

Lamb TD (1995). Photoreceptor spectral sensitivities: common shape in the long-wavelength region. *Vision Res* **35**, 3083–3091.

Levenson DH, Fernandez-Duque E, Evans S & Jacobs GH (2007). Mutational changes in S-cone opsin genes common to both nocturnal and cathemeral *Aotus* monkeys. *Am J Primatol* **69**, 757–765.

Leventhal AG, Rodieck RW & Dreher B (1981). Retinal ganglion cell classes in the Old World monkey: morphology and central projections. *Science* **213**, 1139–1142.

Marrocco RT & Li RH (1977). Monkey superior colliculus: properties of single cells and their afferent inputs. *J Neurophysiol* **40**, 844–860.

Martin PR, Blessing EM, Buzás P, Szmajda BA & Forte JD (2011). Transmission of colour and acuity signals by parvocellular cells in marmoset monkeys. *J Physiol* **589**, 2795–2812.

Martin PR, White AJR, Goodchild AK, Wilder HD & Sefton AE (1997). Evidence that blue-on cells are part of the third geniculocortical pathway in primates. *Eur J Neurosci* **9**, 1536–1541.

Moors J & Vendrik AJ (1979). Responses of single units in the monkey superior colliculus to moving stimuli. *Exp Brain Res* **35**, 349–369.

Ogasawara K, McHaffie JG & Stein BE (1984). Two visual corticotectal systems in cat. *J Neurophysiol* **52**, 1226–1245.

Perry VH & Cowey A (1984). Retinal ganglion cells that project to the superior colliculus and pretectum in the macaque monkey. *Neuroscience* **12**, 1125–1137.

Perry VH, Oehler R & Cowey A (1984). Retinal ganglion cells that project to the dorsal lateral geniculate nucleus in the macaque monkey. *Neuroscience* **12**, 1101–1123.

Petrusca D, Grivich MI, Sher A, Field GD, Gauthier JL, Greschner M, Shlens J, Chichilnisky EJ & Litke AM (2007). Identification and characterization of a Y-like primate retinal ganglion cell type. *J Neurosci* **27**, 11019–11027.

Rodieck RW & Dreher B (1979). Visual suppression from nondominant eye in the lateral geniculate nucleus: a comparison of cat and monkey. *Exp Brain Res* **35**, 465–477.

Rodieck RW & Watanabe M (1993). Survey of the morphology of macaque retinal ganglion cells that project to the pretectum, superior colliculus, and parvicellular laminae of the lateral geniculate nucleus. *J Comp Neurol* **338**, 289–303.

Roy S, Martin PR, Dreher B, Saalmann YB, Hu D & Vidyasagar TR (2009). Segregation of short-wavelength sensitive (S) cone signals in the macaque dorsal lateral geniculate nucleus. *Eur J Neurosci* **30**, 1517–1526.

Schiller PH & Koerner F (1971). Discharge characteristics of single units in superior colliculus of the alert rhesus monkey. *J Neurophysiol* **34**, 920–936.

Schiller PH & Malpeli JG (1977). Properties and tectal projections of monkey retinal ganglion cells. *J Neurophysiol* **40**, 428–445.

Schiller PH & Malpeli JG (1978). Functional specificity of lateral geniculate nucleus laminae of the rhesus monkey. *J Neurophysiol* **41**, 788–797.

Schiller PH & Stryker M (1972). Single-unit recording and stimulation in superior colliculus of the alert rhesus monkey. *J Neurophysiol* **35**, 915–924.

Sherman SM & Guillery RW (2006). *Exploring the Thalamus and its Role in Cortical Function*. MIT Press, Cambridge, MA.

Skottun BC, DeValois RL, Grosof DH, Movshon JA, Albrecht DG & Bonds AB (1991). Classifying simple and complex cells on the basis of response modulation. *Vision Res* **31**, 1079–1086.

Solomon SG, Tailby C, Cheong SK & Camp AJ (2010). Linear and non-linear contributions to the visual sensitivity of neurons in primate lateral geniculate nucleus. *J Neurophysiol* **104**, 1884–1898.

Sterling P & Wickelgren BG (1969). Visual receptive fields in the superior colliculus of the cat. *J Neurophysiol* **32**, 1–15.

Sumner P, Adamjee T & Mollon JD (2002). Signals invisible to the collicular and magnocellular pathways can capture visual attention. *Curr Biol* **12**, 1312–1316.

Sumner P, Nachev P, Castor-Perry S, Isenman H & Kennard C (2006). Which visual pathways cause fixation-related inhibition? *J Neurophysiol* **95**, 1527–1536.

Sun H, Smithson HE, Zaidi Q & Lee BB (2006*a*). Specificity of cone inputs to macaque retinal ganglion cells. *J Neurophysiol* **95**, 837–849.

Sun H, Smithson HE, Zaidi Q & Lee BB (2006*b*). Do magnocellular and parvocellular ganglion cells avoid short-wavelength cone input? *Visual Neurosci* **23**, 441–446.

Szmajda BA, Buzás P, FitzGibbon T & Martin PR (2006). Geniculocortical relay of blue-off signals in the primate visual system. *Proc Natl Acad Sci U S A* **103**, 19512–19517.

Szmajda BA, Martin PR & Grünert U (2008). Retinal ganglion cell inputs to the koniocellular pathway. *J Comp Neurol* **510**, 251–268.

Tailby C, Dobbie WJ, Hashemi-Nezhad M, Forte JD & Martin PR (2010). Receptive field asymmetries produce color-dependent direction selectivity in primate lateral geniculate nucleus. *J Vision* **10**, 1–18.

Tailby C, Solomon SG, Dhruv NT, Majaj NJ, Sokol SH & Lennie P (2007). A new code for contrast in the primate visual pathway. *J Neurosci* **27**, 3904–3909.

Tailby C, Solomon SG & Lennie P (2008*a*). Functional asymmetries in visual pathways carrying S-cone signals in macaque. *J Neurosci* **28**, 4078–4087.

Tailby C, Szmajda BA, Buzás P, Lee BB & Martin PR (2008*b*). Transmission of blue (S) cone signals through the primate lateral geniculate nucleus. *J Physiol* **586**, 5947–5967.

Tovée MJ, Bowmaker JK & Mollon JD (1992). The relationship between cone pigments and behavioural sensitivity in a New World monkey (*Callithrix jacchus jacchus*). *Vision Res* **32**, 867–878.

Vaney DI & Taylor WR (2002). Direction selectivity in the retina. *Curr Opin Neurobiol* **12**, 405–410.

Webb BS, Dhruv NT, Solomon SG, Tailby C & Lennie P (2005). Early and late mechanisms of surround suppression in striate cortex of macaque. *J Neurosci* **25**, 11666–11675.

White AJR, Goodchild AK, Wilder HD, Sefton AE & Martin PR (1998). Segregation of receptive field properties in the lateral geniculate nucleus of a New-World monkey, the marmoset *Callithrix jacchus*. *J Neurophysiol* **80**, 2063–2076.

White AJR, Solomon SG & Martin PR (2001). Spatial properties of koniocellular cells in the lateral geniculate nucleus of the marmoset *Callithrix jacchus*. *J Physiol* **533**, 519–535.

White BJ, Boehnke SE, Marino RA, Itti L & Munoz DP (2009). Color-related signals in the primate superior colliculus. *J Neurosci* **29**, 12159–12166.

Wickelgren BG & Sterling P (1969). Influence of visual cortex on receptive fields in the superior colliculus of the cat. *J Neurophysiol* **32**, 16–23.

Wiesel TN & Hubel D (1966). Spatial and chromatic interactions in the lateral geniculate body of the rhesus monkey. *J Neurophysiol* **29**, 1115–1156.

Xu X, Ichida JM, Allison JD, Boyd JD, Bonds AB & Casagrande VA (2001). A comparison of koniocellular, magnocellular and parvocellular receptive field properties in the lateral geniculate nucleus of the owl monkey (*Aotus trivirgatus*). *J Physiol* **531**, 203–218.

Author contributions

Experiments were conceived and designed by P.M., C.T. and S.S. Data were collected, interpreted and analysed by all authors. The article was drafted by P.M. and C.T. and revised critically for important intellectual content by all authors. All authors have approved the final version of the manuscript.

Acknowledgements

We thank B. Eriköz, A. Demir and C. Guy for technical assistance and B. Dreher for helpful comments and discussion. This work was supported by an Australian NHMRC grant 1027913 and an Australian Research Council grant CE0561903.